



# IDEALVENT: Characterization of installation effects in aircraft Environmental Control Systems

Christophe SCHRAM<sup>1</sup>; Korcan KUCUKCOSKUN<sup>2</sup>; Julien CHRISTOPHE<sup>3</sup>;

Nicolas VAN DE WYER<sup>4</sup>;

von Karman Institute for Fluid Dynamics, Belgium

## ABSTRACT

Environmental Control System (ECS) are used in order to provide equipment cooling and good thermal comfort for passengers in commercial aircrafts. They are also responsible for significant acoustic annoyance affecting both passengers in the cabin and personnel servicing the aircraft on the ramp. The IDEALVENT project is tackling these issues by proposing a combination of detailed experimental work and advanced simulation techniques to better model, predict and mitigate ECS noise. A specific focus is placed on installation effects, which are addressed through a modular experimental rig permitting various combinations between a blower unit, downstream obstacles and upstream inflow distortions. The preliminary results of the project have permitted highlighting the importance and nature of the aerodynamic and acoustic installation effects that occur in such configurations. This paper is focused on acoustic measurements that have been performed using in-duct microphone arrays. These arrays have been designed to decompose the active and passive components of the blower scattering matrix into a modal basis including up to the first radial mode of the duct.

Keywords: aeroacoustics, ventilation noise, fan noise, installation effects.

## 1. INTRODUCTION

Environmental Control System (ECS) are used in order to provide equipment cooling and good thermal comfort for passengers in commercial aircrafts. One of the key elements of ECS units is the fan, operating in complex duct systems including bends, junctions and restriction diaphragms. The aerodynamic and acoustic interactions between these elements, also called installation effects, can result in substantial acoustic nuisance within the cabin and around the grounded aircraft.

The aerodynamic noise emitted by low-speed rotating machinery applications has been studied extensively by many authors. Tonal fan noise, which appears at discrete frequencies at Blade Passing Frequencies (BPFs) and its harmonics due to the periodic forces applying on the blade surface, has been studied numerically and experimentally [1,2]. In addition, random pressure fluctuations on the blade surface due to turbulence-interaction, boundary layer separation, etc., result in broadband fan noise that has also been the subject of experimental and numerical studies [3-5]. These noise sources can appear even when the fan is operating at its design condition and the sound levels need to be reduced for better passenger and personnel comfort, and due to regulations. Furthermore, it is not always possible to operate the fan in its design conditions. Depending on the resistance in the fan system due to installation effects for example, the fan might operate in off-design conditions, such as stall, surge or free delivery. The first two are mostly due to the increased resistance in the system, such that the fan operates on the low-mass flow rate part of its performance curve. The last one is due to low-resistance in the system, and results in very low pressure difference generated by the fan. The noise generated by the fans operating in off-design conditions has been

---

<sup>1</sup> christophe.schram@vki.ac.be

<sup>2</sup> korcan.kucukcoskun@vki.ac.be

<sup>3</sup> julien.christophe@vki.ac.be

<sup>4</sup> nicolas.vandewyer@vki.ac.be

discussed in previous literature [6-9]. The present study is focused on the particular case of a fan designed for an aircraft ECS.

## 2. EXPERIMENTAL STUDY

### 2.1 Test rig

In order to investigate the aerodynamic sound generated by an ECS fan (provided by Liebherr Aerospace) subjected to installation effects, a modular test-rig has been built at VKI as seen in Figure 1 and Figure 2. The modular structure allows investigating the noise generated by the axial fan including both upstream and downstream installation effects. The rig is schematically represented inside the VKI low-speed fan anechoic room in Figure 1.

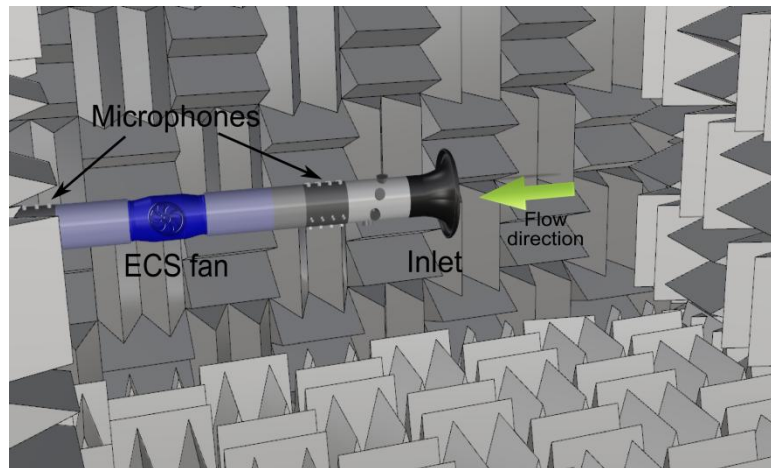


Figure 1 – Schematic representation of the IDEALVENT generic ECS in VKI low-speed fan anechoic room

Figure 2 shows the rig assembled to investigate the effect of downstream obstructions such as diaphragms and valves on the sound generated by the fan. The investigation of upstream installation effects foresees the replacement of the inlet bell-mouth shown below by two different inlets: a T-junction and a rectangular-circular transition. The aerodynamic disturbances associated with each of these inflow devices are characterized by means of a radial-azimuthal hot wire traversing system designed for this project, permitting to measure the velocity magnitude and turbulence intensity over a complete cross-section of the duct.

In this paper we report on the preliminary acoustic measurements performed in these various configurations. The subsequent stages of the IDEALVENT project will deal with the development of simulation strategies permitting to predict the aerodynamic and acoustic interactions between those components.

The ECS fan used in the experimental rig has 15 rotor blades and 10 stator blades and is operated at 11200 rpm. A static frequency converter has been used in order to run the ECS fan in its design conditions. The power-supply converts the three phase input to 115 V and 400 Hz output according to aeronautical standards. There is no voltage nor frequency control on the power supply, therefore the rotational speed is fixed for a given pressure rise. The Blade Passing Frequency (BPF) is equal to 2800 Hz. The fan is operating in a cylindrical plexiglass duct with inner diameter  $D=150$  mm. With this diameter the cut-on frequency for the first azimuthal mode is 1313 Hz. Upstream and downstream ducted microphone modules have been designed and manufactured by KTH, located upstream and downstream of the fan and diaphragm assembly. In total, 32 flush-mounted  $\frac{1}{4}$ -in Bruel & Kjaer 4938-11 high-pressure field microphones and one  $\frac{1}{2}$ -in Bruel & Kjaer 4191 free-field microphones are used. The in-duct microphone sections are used to measure the reflection coefficient downstream of the duct and they will be later used for modal decomposition measurements [10] on the same rig. This paper discusses far-field acoustic measurements performed inside of the anechoic room, in the vicinity of the duct inlet, and the in-duct acoustic measurements.

In order to measure the propagating acoustic waves accurately, the reflected and scattered waves from the downstream open end the duct should be minimized. Therefore, an anechoic termination has been designed and manufactured, consisting of quarter-wave resonators and Micro-Perforated Plates (MPP) fitted at the downstream open end of the duct.

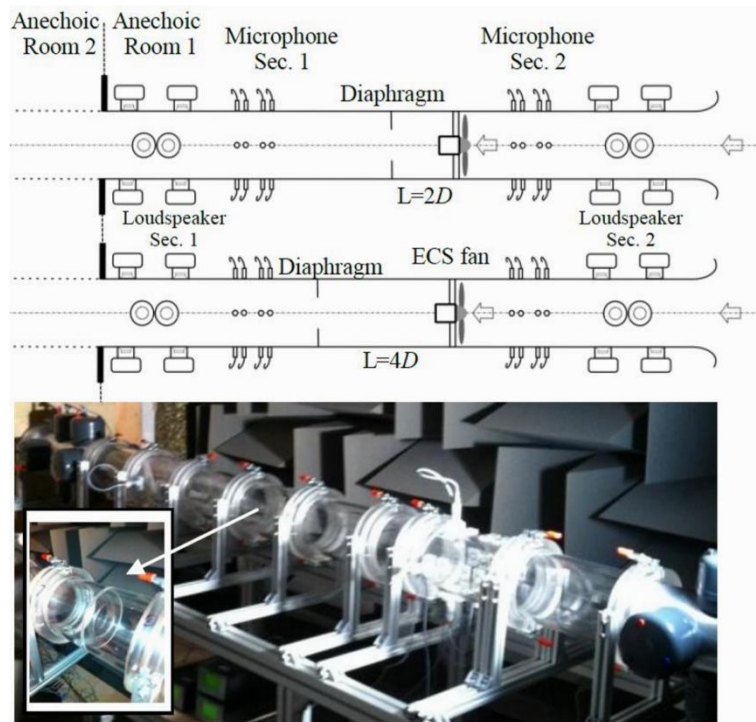


Figure 2 – Modular test rig.

## 2.2 Effect of downstream obstacle

When an obstacle is located downstream of an ECS fan, several installation effects are expected. First of all, the operating point of the fan is altered, which is likely to have an impact on the broadband and tonal contents of the fan sound spectrum. Secondly, the turbulence associated with the turbulent wakes is ingested across the obstacle, causing pressure fluctuations on the latter that radiate in the duct system as well. In our experiments, a diaphragm with two possible aperture diameters ( $0.63D$  and  $0.77D$ ) has been placed downstream of the fan, at two different distances from the fan module ( $2D$  and  $4D$ ). In all results below, the volumetric flow rate is  $0.57 \text{ m}^3/\text{s}$  (corresponding to a bulk velocity equal to  $32 \text{ m/s}$  in the main duct,  $86 \text{ m/s}$  across the  $0.63D$  aperture diaphragm, and  $54 \text{ m/s}$  across the  $0.77D$  aperture diaphragm).

The resulting Sound Pressure Levels (SPL), measured at about  $0.5 \text{ m}$  from the duct inlet and  $45$  degrees from its axis in the anechoic room, are shown in Figure 3 when the  $0.63D$  aperture diaphragm has been used. The spectral shape is preserved in all three cases, suggesting that the additional sound generation mechanism remains with the fan and is not significantly due to wake turbulence ingestion across the diaphragm. A quite substantial increase (up to  $\sim 18 \text{ dB}$ ) is observed in the range  $600 \text{ Hz} - 3 \text{ kHz}$ , reducing to about  $\sim 5 \text{ dB}$  in the highest measured frequencies.

Another point that is worth to note is the modulation of the tonal fan noise in presence of diaphragm. Figure 4 shows a closer look on the first Blade Passing Frequency (BPF) for the fan alone (left), diaphragm at  $4D$  distance (red) and diaphragm at  $2D$  distance (blue). It is seen that in absence of the diaphragm, the acoustic spectra shows a single tone at the BPF. However, introducing the diaphragm downstream the fan, a decrease of the BPF main tone is observed, accompanied by additional modulation tones. For the diaphragm configurations, the shaft rotational frequency is  $189.47 \text{ Hz}$  for  $4D$  and  $189.60 \text{ Hz}$  for  $2D$ . The modulation frequency step is  $102 \text{ Hz}$  for all configurations, and was shown to be due to fan surge and possibly rotating stall. Indeed, the rotating stall frequency has been reported between  $30\%$  and  $80\%$  of the shaft rotational frequency in previous studies [7, 9]. In this configuration, the modulation frequency is  $55\%$  of the shaft rotational frequency and rotating stall can explain the modulation of the tonal fan noise.

The results obtained with the diaphragm having  $0.77D$  aperture diameter illustrate that in absence of rotor surge, the increase of SPL is much more moderate (Figure 5). A global increase of the levels of the order of  $2\text{-}3 \text{ dB}$  can be seen at frequencies below  $\sim 1 \text{ kHz}$ , but they remain overall unchanged at higher frequencies. It should be stressed that the previous operating point, corresponding to rotating stall and surge, is clearly out of the normal design and operational range of the fan used in this work.

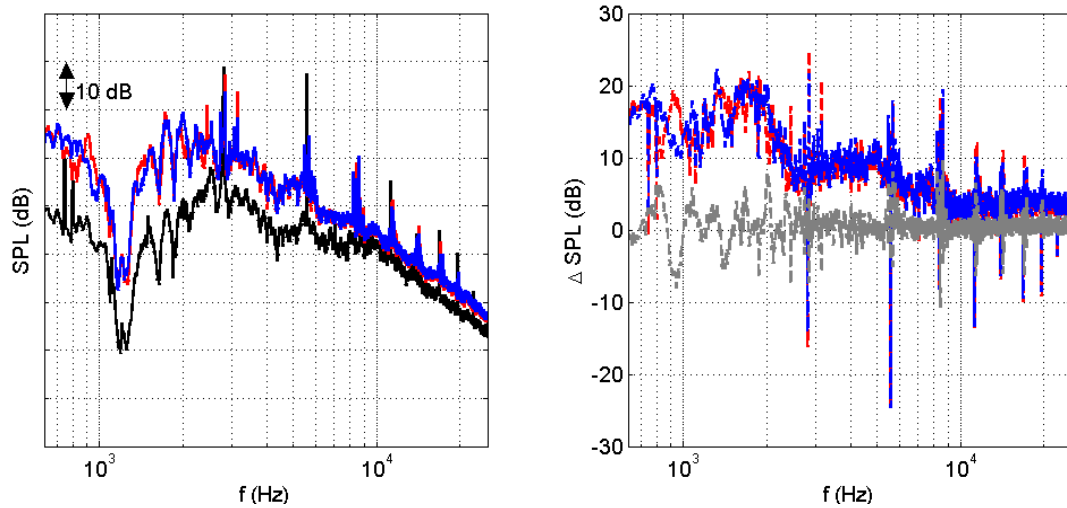


Figure 3 – SPL measured in the anechoic room (at about 0.5 m from the duct inlet and 45 degrees from its axis) for the ECS fan placed in empty duct (black), at 2D upstream of the 0.63D aperture diaphragm (blue) and at 4D upstream of the 0.63D aperture diaphragm (red). Left: absolute levels, right: delta-dB levels (blue: between diaphragm at 2D and no-diaphragm, red: between diaphragm at 4D and no-diaphragm, gray: between diaphragm at 2D and diaphragm at 4D).

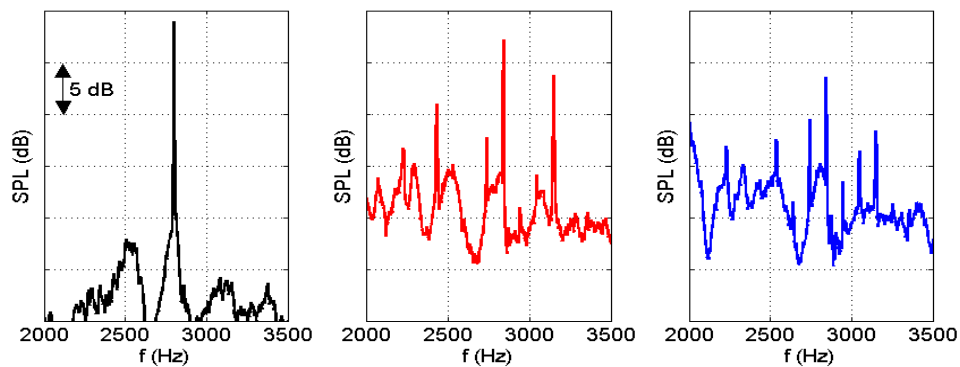


Figure 4 – SPL measured in the anechoic room for the ECS fan placed in empty duct (left), at 4D upstream of the 0.63D aperture diaphragm (middle) and at 2D upstream of the 0.63D aperture diaphragm (right).

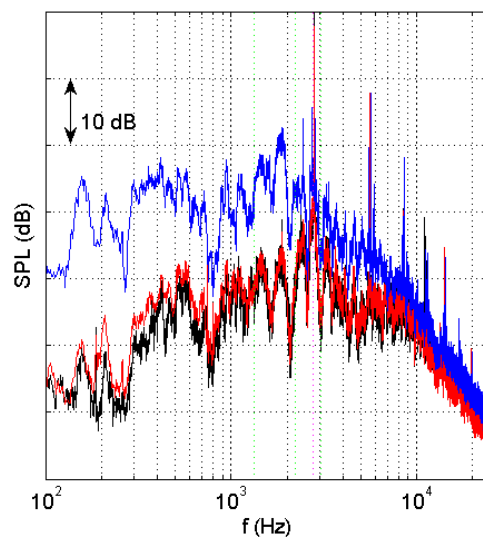


Figure 5 – SPL measured in the anechoic room for the ECS fan placed in empty duct (black), at 4D upstream of the 0.63D aperture diaphragm (blue), at 4D upstream of the 0.77D aperture diaphragm (red).

### 2.3 Effect of inflow distortions

Another point addressed in the IDEALVENT project is the ECS fan operating in presence of upstream disturbances. A T-junction and a rectangular-to-circular transition modules have been manufactured, representative of complex ECS duct components in realistic operating environments. Figure 6 shows the Plexiglas inlet modules manufactured at VKI. The T-junction (left) consists of two symmetrical inlets where the areas of each inlet are equal to the one of outlet. Both inlet radii and the outlet radius are equal to 75 mm. The inlets are smoothly connected to the outlet via a tongue in the T-junction module. The rectangular to circular transition module (right) has a smooth transition between inlet and outlet. The inlet area is equal to the two times the outlet area. The length of the horizontal edge of the rectangular inlet is twice the vertical one.



Figure 6 – Inlet distortion modules (left: T-junction, right: rectangular-circular transition)

In the far-field measurements, a ½” B&K microphone is used, located at the suction side of the anechoic room. The inlet modules are located at  $4D$  upstream of the fan. Figure 7 shows the free-field SPL (left) measured at the inlet of the modules. The center-line flow velocity is equalized to about 32 m/s for all three cases which is satisfied by using the auxiliary fan similar to the ones presented above. The black, red and blue represent results obtained with the bell-mouth, the T-junction and the rectangular-circular transition modules, respectively. It is seen that the lowest sound levels have been obtained in clean inlet conditions using the bell-mouth. Introducing the rectangular-circular transition and the T-junction modules, the sound pressure levels are increased around 5 dB and 15 dB at low frequencies, respectively. It should be noted that the sound generated by the fan is first propagated inside the duct and later reflected and scattered by the inlet modules before it reaches to the microphone. In presence of the T-junction especially, the microphone can be located in a quiet zone. Therefore additional in-duct measurements are performed for the fan operating in presence of inlet distortion. Figure 7 (left) shows the SPL of obtained through in-duct measurements (right) performed downstream of the ECS fan. Similarly, using the transition and T-junction modules increase the sound pressure levels at lower frequencies around 5 dB and 15 dB, respectively. The first and second axial cut-on modes can be seen clearly in the figure around 1300 Hz and 2200 Hz, respectively. The levels associated to the BPFs don't show significant alterations, in comparison with the broadband increase.

This has been measured by means of the hot-wire radial-azimuthal traversing system. The results are shown in Figure 8 for the mean velocity field measured  $1D$  downstream of the flange connecting the inlet module to the main pipe. It can be seen that while the bell-mouth inlet guarantees a good inflow azimuthal homogeneity (left), strong azimuthal distortions are induced by the T-junction (middle) and rectangular-circular transition (right). These results are being further analyzed in a view to serve as inflow boundary conditions for semi-analytical and numerical modeling approaches, in the next steps of the project.

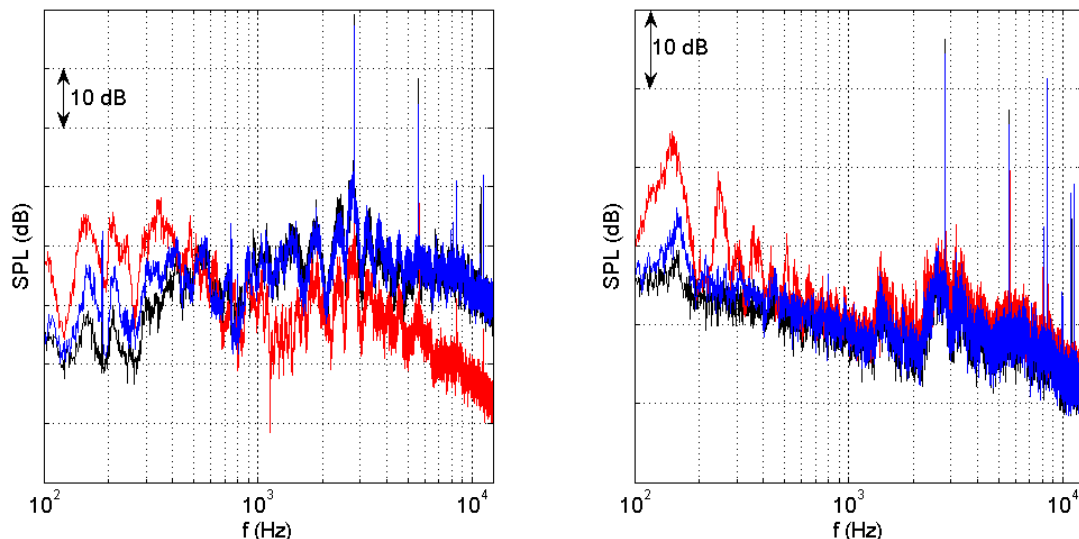


Figure 7 – SPL of ECS fan operating in presence of different inlet modules (black: with bell-mouth inlet; red: with T-junction inlet; blue: with rectangular-circular transition inlet). Left: microphone in the anechoic room at about 0.5 m from the duct inlet and 45 degrees from its axis; right: in-duct microphone

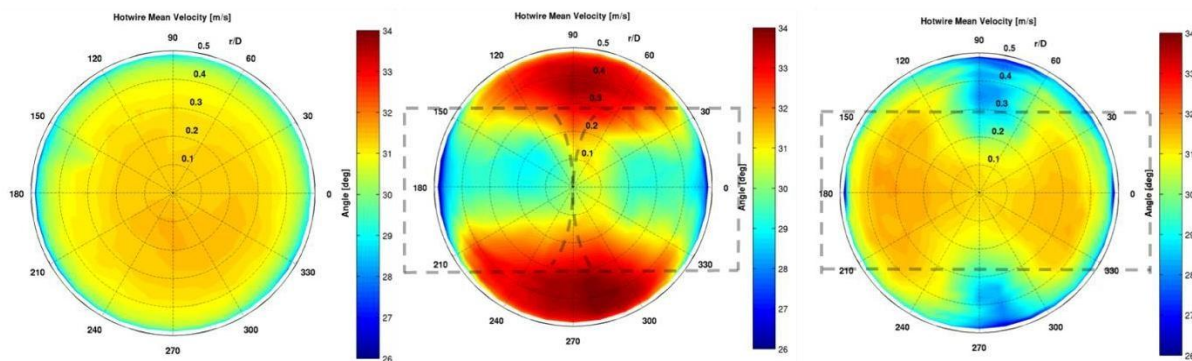


Figure 8 – Mean flow velocity in a cross-plane located downstream of the connection of the different inlet modules (left: bell-mouth; middle: T-junction; right: rectangular-circular transition)

### 3. Summary and perspectives

The IDEALVENT project is aimed at providing a better understanding of aero-acoustic installation effects in ventilation systems, with a focus on aircraft Environmental Control Systems. A dedicated rig has been designed and assembled to this end, in the VKI low-speed fan anechoic room. The rig is equipped with free-field and in-duct microphones and permits the characterization of cross-plane hot-wire traverses. Two types of installation effects have been investigated: when an obstacle is located downstream of the fan, and when inflow distortions are ingested by the fan.

The preliminary results indicate that in presence of a downstream diaphragm with too small aperture diameter, the sound emitted by the axial blower can dramatically increase, especially in the low frequencies, due to rotor surge and rotating stall. When the pressure loss across the diaphragm is reduced to avoid stall, only a minor increase of the fan noise is observed. In either case, the additional noise is conjectured to be due to the fan operating point alteration, rather than due to the ingestion of the fan wakes turbulence across the diaphragm.

When an inflow distortion is introduced, by means of a T-junction or rectangular-circular transition in the present study, significant additional broadband noise is produced by the fan, mainly in the low-frequency broadband region. The comparatively minor alteration of the BPF tones was somehow not expected, and will require further explanations.

In the next steps of the project, various modeling approaches such as semi-analytical (based on Amiet's theory) and numerical methods (URANS) will be applied to these configurations, in order to validate the modeling assumptions and bring further clarification of the experimental observations.

## ACKNOWLEDGEMENTS

The authors gratefully acknowledge the support of the European Commission, provided in the framework of the FP7 Collaborative Project IDEALVENT (Grant Agreement no 314066). The microphone array used for the in-duct measurements was designed and manufactured by KTH (Stockholm) under guidance of Mats Abom and Stefan Sack, and their precious advises and contributions are gratefully acknowledged as well. Liebherr Aerospace has kindly provided the fan unit that is used in the IDEALVENT project.

## REFERENCES

- [1] Farassat, F., Succi, G.P., 1980, "A review of propeller discrete frequency noise prediction technology with emphasis on two current methods for time domain calculations", *Journal of Sound and Vibration*, 71(3):399-419.
- [2] Goldstein, M., 1976, *Aeroacoustics*, Mc-Graw Hill, New-York.
- [3] Carolus, T., Schneider, M., Reese, H., 2007, "Axial flow broadband noise and prediction", *Journal of Sound and Vibration*, 300(1-2):50-70.
- [4] Rozenberg, Y., Roger, M., Moreau, S., 2010, "Rotating Blade Trailing-Edge Noise: Experimental Validation of Analytical Model", *AIAA Journal*, 48(5):951-962.
- [5] Moreau, S., Roger, M., 2007, "Competing broadband noise mechanisms in low speed axial fans", *AIAA Journal*, 45(1):45-57.
- [6] Cho, Y., Moon, Y.J., 2003, "Discrete noise prediction of variable pitch cross-flow fans by unsteady Navier-Stokes computations", *Journal of Fluids Engineering*, 125:543-550.
- [7] Mongeau, L., Thompson, D.E., McLaughlin, D.K., 1993, "Sound generation by rotating stall in centrifugal turbomachines", *Journal of Sound and Vibration*, 163(1):1-30.
- [8] Gerard, A., Moreau, S., Berry, A. Masson, P., 2012, "Acoustic modulation effect of rotating stator/rotor interaction noise", *Proceedings of the Acoustics 2012 Nantes Conference*, 3781-3786.
- [9] Dong, G., Zhong, F., 1990, "The analysis of sound field and flow field of low pressure axial flow fan in rotating stall", *First International Symposium of Experimental and Computational Aerothermodynamics of Internal Flows*, 647-651.
- [10] Lavrentjev, J., Abom, M., Boden, H., 1995, "A measurement method for determining the source data of acoustic two-port sources", *Journal of Sound and Vibration*, 183(3):517-531.